



UNIVERSITY OF LEEDS

This is a repository copy of *2D networks of metallo-capsules and other coordination polymers from a hexapodal ligand*.

White Rose Research Online URL for this paper:

<https://eprints.whiterose.ac.uk/132428/>

Version: Accepted Version

---

**Article:**

Thorp-Greenwood, FL orcid.org/0000-0001-6228-2056, Berry, GT, Boyadjieva, SS et al. (2 more authors) (2018) 2D networks of metallo-capsules and other coordination polymers from a hexapodal ligand. *CrystEngComm*, 20 (28). pp. 3939-4060. ISSN 1466-8033

<https://doi.org/10.1039/C8CE00806J>

---

(c) The Royal Society of Chemistry 2018, This is an author produced version of a paper published in *CrystEngComm*. Uploaded in accordance with the publisher's self-archiving policy.

**Reuse**

Items deposited in White Rose Research Online are protected by copyright, with all rights reserved unless indicated otherwise. They may be downloaded and/or printed for private study, or other acts as permitted by national copyright laws. The publisher or other rights holders may allow further reproduction and re-use of the full text version. This is indicated by the licence information on the White Rose Research Online record for the item.

**Takedown**

If you consider content in White Rose Research Online to be in breach of UK law, please notify us by emailing [eprints@whiterose.ac.uk](mailto:eprints@whiterose.ac.uk) including the URL of the record and the reason for the withdrawal request.



[eprints@whiterose.ac.uk](mailto:eprints@whiterose.ac.uk)  
<https://eprints.whiterose.ac.uk/>



## 2D networks of metallo-capsules and other coordination polymers from a hexapodal ligand

Flora L. Thorp-Greenwood,<sup>a</sup> Gilberte Therese Berry,<sup>a</sup> Sophia S. Boyadjieva,<sup>a,b</sup> Samuel Oldknow,<sup>a</sup> and Michael J. Hardie<sup>\*a</sup>

Received 00th January 20xx,  
Accepted 00th January 20xx

DOI: 10.1039/x0xx00000x

www.rsc.org/

The hexapodal ligand hexakis(isonicotinoyl)cyclotrivatechylene (L1) belonging to the cyclotrivatechylene family of host-molecules has been synthesised and used in the assembly of a series of coordination polymer materials with Re(I), Co(II), Cu(II), Ni(II) and Ag(I) salts. Single crystal structures of the coordination polymers [Re<sub>3</sub>(L1)<sub>2</sub>Br<sub>3</sub>(CO)<sub>3</sub>] **1**, and an isomorphous [M<sub>3</sub>L<sub>2</sub>] series where M = Co, Cu or Ni, reveal 2D framework structures with a simplified topology of 3<sup>6</sup> or **hxl**. These are composed of M<sub>6</sub>(L1)<sub>2</sub> metallo-cages linked together in a pair-wise fashion through each metal centre. Compound **1** is a rare example of a rhenium coordination polymer and was investigated for guest uptake from solution, complexing I<sub>2</sub>. The mixed-ligand species [Cu<sub>2</sub>(L1)(CF<sub>3</sub>CO<sub>2</sub>)<sub>3</sub>(isonicotinate)] forms a (3,4,5)-connected 2D coordination polymer, while [Ag<sub>2</sub>(L1)(DMF)<sub>2</sub>·2BF<sub>4</sub>·2(H<sub>2</sub>O)·6(DMF)] features a 2D network of (3,6)-connectivity and with kagome dual (kgd) topology.

### Introduction

Coordination polymers (CPs) and metal-organic frameworks (MOFs) are well-ordered polymeric coordination compounds.<sup>1</sup> MOFs and many coordination polymers are robust porous materials, which is a function of the structural assembly of metal ion and ligand. This has led to a raft of potential applications for these materials including in gas storage, separations, drug delivery and catalysis which is often predicated on the ability of CPs and MOFs to bind guest molecules within their pores.<sup>1,2</sup> Molecular hosts are individual molecules that have an intrinsic ability to bind guest molecules. Most examples are cyclic or cage-like in nature. The use of molecular hosts as components of coordination polymers<sup>3-18</sup> is notable as it may result in a material with hierarchical pore space through both the specific molecular recognition sites of the molecular host, and lattice channels and cavities of the coordination polymer framework. One class of hosts are those with a bowl-like conformation of the macrocycle with shallower lower-rim and more expansive upper rim. Examples of such hosts include calix[4]arenes, resorcinarenes and cyclotrivatechylenes. When these hosts are functionalised with suitable metal-binding groups then they may form coordination polymers,<sup>4-18</sup> or discrete metallo-capsule and metallo-cage assemblies.<sup>19</sup> Combining both assembly behaviours to form coordination polymers composed of linked metal-

capsules/cages is an attractive proposition as it potentially creates materials with pre-defined cavities.<sup>6-14</sup> Functionalised pre-formed organic cages can also be used to form coordination polymers.<sup>20</sup> It also avoids situations where unwanted host-guest interactions – such as self-inclusion motifs of hosts or networks - effectively block the host molecular cavity from any subsequent functionality.<sup>5,16,17</sup> Networks of M<sub>n</sub>L<sub>2</sub> metallo-capsules where L is a bowl-shaped host ligand have been reported for chain assemblies, and 2D networks using functionalised calix[4]arenes,<sup>6</sup> resorcinarenes,<sup>7</sup> pyrogallol[4]arenes,<sup>8,9</sup> and tripodal cyclotrivatechylene analogues.<sup>10-12</sup> Networks of larger metallo-cages have also been reported.<sup>13,14</sup>

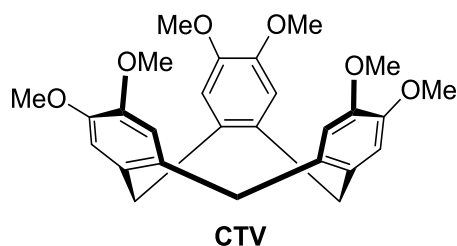
Our work focuses on the use of molecular hosts of the cyclotrivatechylene (CTV) family that have been functionalised at the upper rim with metal-binding groups. CTV and related hosts have a tribenzo[*a,d,g*]cyclononene scaffold and their thermodynamically stable crown conformation affords a bowl-like cavity. We, and others, have concentrated on formation of coordination polymers with tripodal C<sub>3</sub>-symmetric CTV-analogues where there are three ligand moieties.<sup>10-12,15-18</sup> Examples of linked metallo-capsules with CTV-ligands are rare and include a [Cu<sub>3</sub>L<sub>4</sub>]-6OTf coordination polymer material where L = *tris*(isonicotinoyl)cyclotrivaigaiacyclene. This is composed of Cu<sub>3</sub>L<sub>2</sub> metallo-capsules that are linked together at the Cu(II) centres to form a 2D hexagonal network with simplified 6<sup>3</sup> **hcb** topology taking the capsule as the network node.<sup>10</sup> The structure contained very large channels and could bind fullerene-C<sub>60</sub> from solution, but was not robust and becomes amorphous removal of solvent. CTV-type metallo-capsule-based networks of same topology have also been reported with Ag-Cl-Ag linkers,<sup>11</sup> and in a MOF recently reported by Easun and co-workers where a hexagonal network is formed

<sup>a</sup> School of Chemistry, University of Leeds, Woodhouse Lane, Leeds LS2 9JT, UK.  
email: m.j.hardie@leeds.ac.uk

<sup>b</sup> Current address: School of Chemistry, University of Glasgow, Glasgow G12 8QQ, UK

† Footnotes relating to the title and/or authors should appear here.

Electronic Supplementary Information (ESI) available: CCDC 1823164-1823172. NMR, MS, IR spectra, TGA traces, microanalysis and EDX, additional figures of crystal structures, and crystallographic data in CIF format. See DOI: 10.1039/x0xx00000x



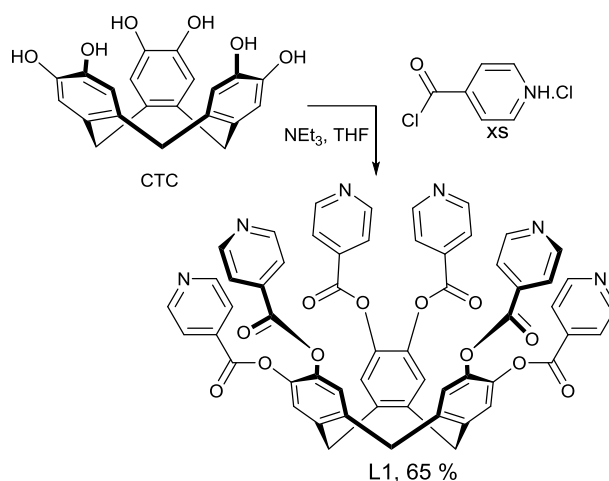
from carboxylate tripodal CTV-type ligand.<sup>12</sup>

These examples all employ tripodal CTV-type ligands, and there has been very little attention given to the development of hexapodal CTV ligands for metallo-supramolecular or coordination chemistry, although it should be noted that demethylated CTV is a catecholate, and can bind transition metals.<sup>14,21</sup> Indeed to the best of our knowledge the only examples of such metal complexes with extended ligand groups are trinuclear Cu(II/I) complexes of a *hexakis*(bipyridyl)-CTV reported by Weiss and Gross and coworkers,<sup>22</sup> and trinuclear complexes of a *hexakis*(2-pyridyl)-CTV.<sup>23</sup> A small number of additional hexakis-substituted CTVs with good transition metal binding groups are also known.<sup>24,25</sup> We report herein a new hexapodal-CTV ligand, namely *hexakis*(isonicotinoyl)cyclotriccatechylene, L1, and a series of coordination polymer materials that were obtained from it. The majority of these feature  $M_6L_2$  metallo-capsule motifs linked into a 2D polymer network.

## Results and discussion

The novel hexa-functionalised ligand *hexakis*(isonicotinoyl)cyclotriccatechylene, L1 (systematic name 4-pyridinecarboxylic acid, 10,15-dihydro-5*H*-tribenzo[*a,d,g*]cyclononene-2,3,7,8,12,13-hexayl ester), was synthesised in 65 % yield from reaction of cyclo-triccatechylene (CTC) with isonicotinoyl chloride hydrochloride in the presence of  $NEt_3$ , Scheme 1. Yields of the desired hexa-substituted are maximised by addition of a large excess of  $NEt_3$  to CTC and stirring at 0 °C for an hour prior to addition of excess isonicotinoyl chloride hydrochloride. Compared with our previous reported synthesis of the isomeric *hexakis*(nicotinoyl)cyclotriccatechylene,<sup>24</sup> the successful synthesis of L1 requires a much larger excess of  $NEt_3$ . The <sup>1</sup>H NMR spectrum of L1 gives the anticipated simple spectrum for a symmetric product with two doublets for the bridging methylene groups, which is characteristic of bowl-shaped tribenzo[*a,d,g*]cyclononene. Peaks corresponding to  $\{M+H\}^+$ ,  $\{M+2H\}^{2+}$  and  $\{M+3H\}^{3+}$  species were all observed in the mass spectrum.

The crystal structure of the crystalline solvate L1·DMF (DMF = dimethylformamide) was obtained using synchrotron radiation. The structure was solved in the triclinic space group  $P\bar{1}$  and the asymmetric unit comprises one complete L1 molecule and a DMF with one methyl group directed into the hydrophobic L1 bowl, Fig. 1. The orientation of the six isonicotinoyl groups of L1 are all quite distinct, and a displaced capsule motif is formed by inverted pairs of host and guest, Figure 1b. There are few examples of crystal structures of hexa-substituted CTC-type compounds (excluding CTC complexes).



Scheme 1 Synthesis of L1.

This is the first to show guest solvent as the intra-cavity guest, with other examples forming self-inclusion motifs.<sup>20,21</sup>

## Rhenium-linked Coordination Polymer

Solvothermal reaction of L1 with  $Re(CO)_5Br$  in nitromethane at 60 °C yields the crystalline coordination polymer compound

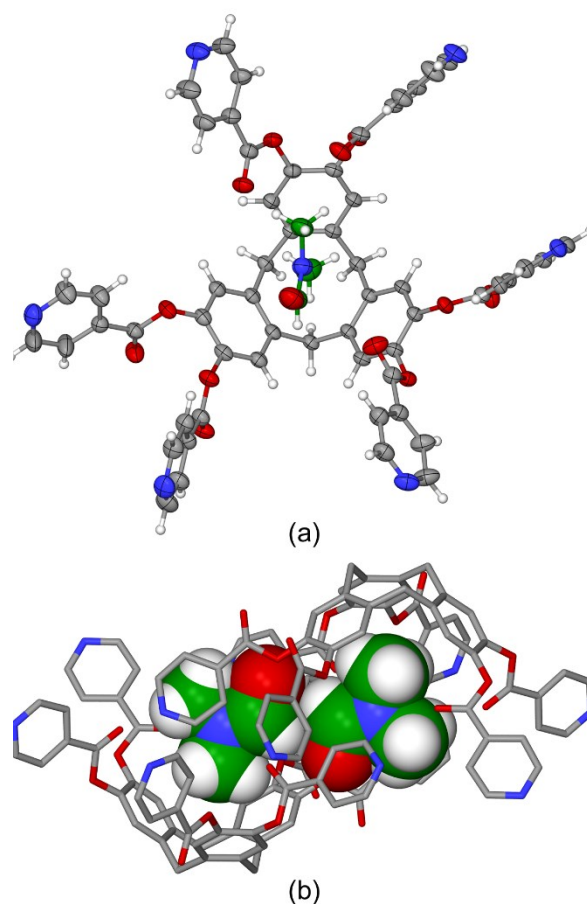
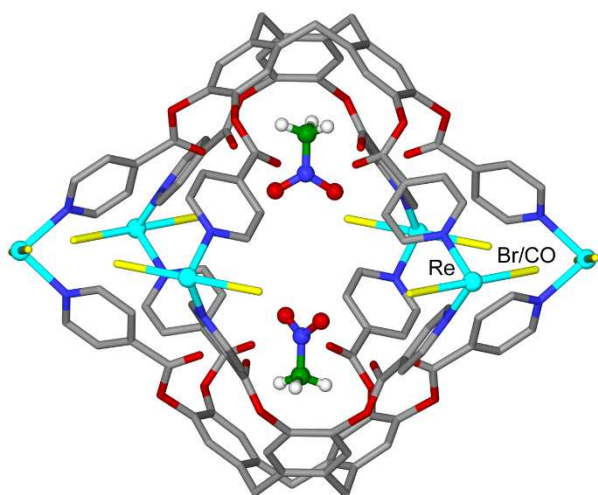


Fig. 1 Crystal structure of L1·DMF. (a) Asymmetric unit with ellipsoids shown at 50 % probability levels; (b) dimeric displaced capsule motif with DMF guest in space-filling.

$[\text{Re}_3(\text{L}1)_2\text{Br}_3(\text{CO})_3] \cdot n(\text{CH}_3\text{NO}_2) \cdot m(\text{H}_2\text{O})$  **1**. The crystal structure of **1** was determined in the trigonal space group  $R\bar{3}m$ . The asymmetric unit comprises one sixth of the L1 ligand, Re(I) and Br on special positions, water and nitromethane solvent also on symmetry positions. The L1 ligand is located around an axis of  $3m$  symmetry, thus the orientation of all six isonicotinoyl groups are symmetry-related with the carbonyl groups oriented inwards with regards to the molecular cavity of L1. Each isonicotinoyl group binds to a Re(I) centre at Re-N distance 2.199(9) Å. A capsule-like motif is formed by two L1 ligands coming together in a head-to-head fashion and coordinating to six Re(I) centres, Fig. 2. The two L1 ligands of this capsule are in a staggered arrangement and the distance between their lower-rims (defined as centre of the three methylene bridges) is 16.3 Å. The six Re(I) centres are at the equator of the capsule and form a perfect hexagon with closest Re...Re separations of 9.83 Å. The hydrophobic  $-\text{CH}_3$  groups of nitromethane guest molecules are directed into the molecular bowl of each L1 ligand at 3.96 Å between the nitromethane C atom and the lower-rim of L1, Fig. 2. The coordination sphere of each Re is distorted octahedral and comprises four isonicotinoyl groups from four symmetry-equivalent L1 ligands, and two terminal and symmetry-equivalent ligands of mixed Br/CO character in a *trans* arrangement. The terminal ligand position was refined as half Br as the superimposed disordered CO could not be adequately refined and was thus excluded from the model. Its presence, however, is evident in the infrared (IR) spectrum of **1** with a  $\nu_{\text{CO}}$  stretch at 2024  $\text{cm}^{-1}$ .

Each  $[\text{Re}_6\text{Br}_6(\text{CO})_6(\text{L}1)_2]$  capsule connects to six other capsules via the Re(I) centres giving a 2D coordination polymer of composition  $[\text{Re}_3\text{Br}_2(\text{CO})_6(\text{L}1)_2]$ , Fig. 3a. If each  $[\text{Re}_6\text{Br}_6(\text{CO})_6(\text{L}1)_2]$  capsule is considered a single 6-connecting centre for the network then a simplified topology is the  $3^6$  **hxl** hexagonal lattice.<sup>26</sup> The network features both the pore space



**Fig. 2** From the crystal structure of  $[\text{Re}_3(\text{L}1)_2\text{Br}_3(\text{CO})_3] \cdot 2(\text{CH}_3\text{NO}_2) \cdot 6(\text{H}_2\text{O})$  **1**.  $[\text{Re}_6\text{Br}_6(\text{CO})_6(\text{L}1)_2]$  capsule-like motif of **1**, with guest  $\text{CH}_3\text{NO}_2$ . Complete Re coordination spheres are not shown and each Br position (in yellow) is actually an averaged Br/CO ligand. Only one position for each of the symmetry-disordered  $\text{CH}_3\text{NO}_2$  is shown for the sake of clarity.

inherent in the capsule motif and has triangular spaces partially occupied by the Br/CO ligands. In previous examples of 2D networks of linked  $\text{M}_3\text{L}_2$  metallo-capsules with tripodal-CTV type ligands the capsules were linked in a trigonal fashion to give a hexagonal  $6^3$  network of **hcb** topology.<sup>10-12</sup> The **hxl** topology is not common and requires a hexagonal linking unit. Known examples include networks where bridging ligand has pyridine-*N*-oxide donors which allow bent N-O-M coordination angles,<sup>27</sup> metal clusters acting as the hexagonal linker,<sup>28</sup> and Atwood's 2D networks of metal-seamed nanocapsules.<sup>8,13</sup> The latter involve  $\text{Ni}_{24}\text{L}_6$  nanocapsules where L is a host pyrogallol[4]arene that has been decorated with hydroxyl groups which bind to Ni(II) centres of adjacent nanocapsule to form the **hxl** network,<sup>13</sup> and  $\text{Zn}_8\text{L}_2$  capsules linked by bridging 4,4'-bipyridine.<sup>8</sup>

In **1** the 2D layers pack such that the capsule motif of one layer is located above the triangular space of an adjacent layer, Fig. 3b. There are small channels through the crystal lattice and inspection of a void map (Fig. 3c) shows that the pores created by the capsule-motifs are connected together by channels. If solvent positions are excluded from the structure then the total void space within the crystal lattice is ca. 30 % of the unit cell volume. While some solvent positions were located by crystallographic analysis, the actual level of solvation of as-synthesised **1** is likely to be higher. Thermal gravimetric analysis (TGA) was used to estimate the solvation levels, and indicates a 15 % weight loss between room temperature and 100 °C attributable to loss of solvent. This corresponds to ca. seven  $\text{CH}_3\text{NO}_2$  and six  $\text{H}_2\text{O}$  per cage-unit or eight to nine  $\text{CH}_3\text{NO}_2$ . The material is otherwise thermally stable, decomposing above 320 °C, Fig. S15 (ESI).

The use of rhenium as a linker metal for a coordination polymer is rare, and the majority of examples feature Re clusters<sup>29</sup> rather than an isolated Re(I) as here. Metallo-ligands decorated with  $\text{Re}(\text{CO})_n\text{X}$  groups have been used to for MOFs/CPs in order to introduce photochemical properties.<sup>30</sup> Compound **1** is pale yellow in colour. Therefore a preliminary assessment of the ability of them to take up guest molecules can be performed simply by soaking the crystals in solutions containing dyes. Unlike  $[\text{Cu}_3\text{L}_4] \cdot 6\text{OTf}$ ,<sup>10</sup> **1** does not take up fullerene- $\text{C}_{60}$  which is as anticipated from the much smaller channel size. However, soaking the crystals in toluene solutions of indigo, rhodamine or iodine led to colour changes in the crystals. This was determined to be only a surface effect for indigo and rhodamine, however incorporation of iodine into the crystals was effected, Fig. 4. While the samples remained crystalline they were not of sufficient quality for single crystal X-ray analysis. TGA indicates no change to the thermal stability of the material post iodine-exposure, Fig. S15. SEM-EDX analysis indicates significant uptake of  $\text{I}_2$ . Both single crystal particles and a ground sample were measured and gave comparable Re:I ratios of  $\text{ReI}_{0.56}$  and  $\text{ReI}_{0.52}$  respectively. This equates to approximately 1.5  $\text{I}_2$  molecules per cage-construct, and indicates that the  $\text{I}_2$ -uptake is not simply a surface effect. We have previously reported the up-take of  $\text{I}_2$  by a crystalline lattice of discrete metallo-cryptophane cage species in a single-crystal-to-single-crystal fashion. There, structure determination

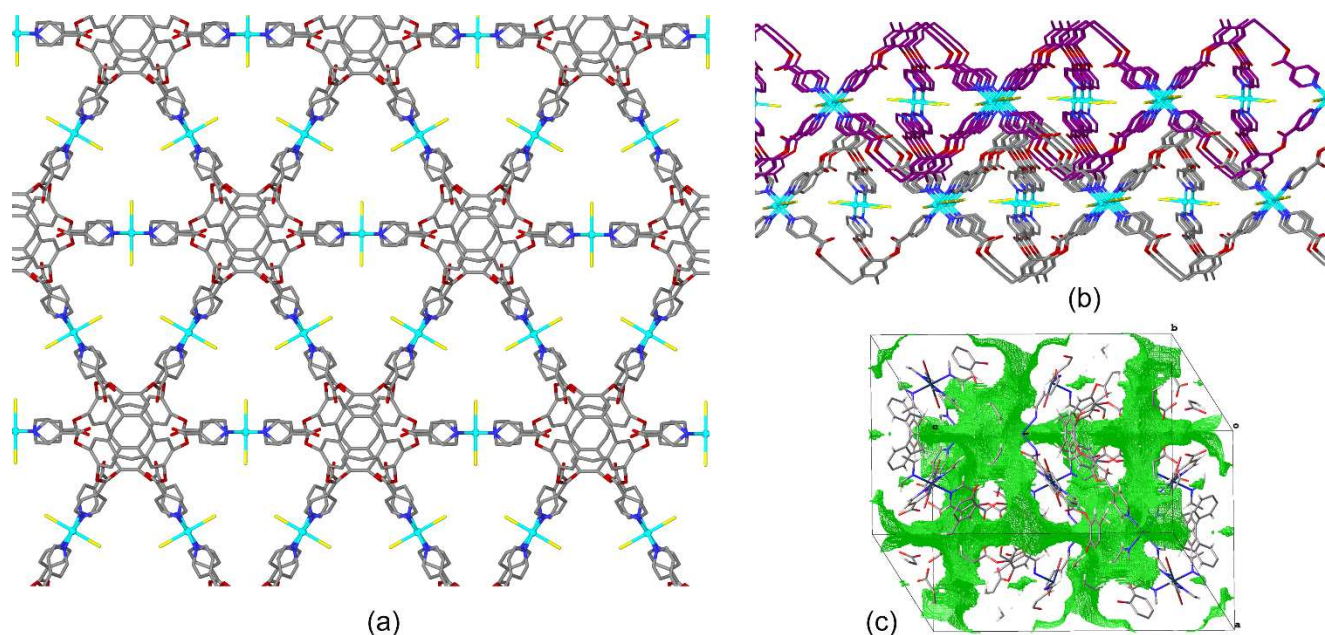


**Fig. 3** From the crystal structure of  $[\text{Re}_3(\text{L1})_2\text{Br}_3(\text{CO})_3] \cdot 2(\text{CH}_3\text{NO}_2) \cdot 6(\text{H}_2\text{O})$  **1**. (a)  $[\text{Re}_3\text{Br}_3(\text{CO})_3(\text{L1})_2]$  network of **hxl** topology; (b) packing of two 2D networks; (c) unit cell void map, green mesh indicates surface of void space when solvent is excluded.

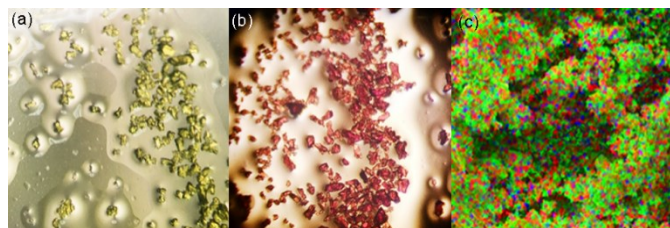


**Fig. 4** Optical and electron microscopy images of (a) as-synthesised compound  $[\text{Re}_3(\text{L1})_2\text{Br}_3(\text{CO})_3] \cdot n(\text{CH}_3\text{NO}_2) \cdot m(\text{H}_2\text{O})$  **1**; (b) **1** after uptake of iodide from toluene solution; (c) SEM-EDX image showing element mapping for ground sample, green = I; red = Re, blue = Br.

showed the  $\text{I}_2$  bound within the cage structures.<sup>31</sup> A number of other cage or macrocycle<sup>32</sup> and MOF-type materials<sup>33</sup> are also able to bind  $\text{I}_2$  as a guest.

### Isostructural Coordination Polymers

Reaction of L1 with a variety of first row transition metal salts in DMF yields crystalline coordination polymer materials with  $\text{M}_3(\text{L1})_2$  stoichiometry. The materials are isostructural and have a 2D coordination polymer structure of linked  $\text{M}_6\text{L}_2$  capsules that is topologically the same as that seen in the coordination polymer compound **1** but in a lower-symmetry structure. Single crystals of materials  $[\text{M}_3(\text{H}_2\text{O})_6(\text{L1})_2] \cdot 6(\text{NO}_3) \cdot n(\text{DMF})$  where  $\text{M} = \text{Co}(\text{II})$  **2a**,  $\text{Cu}(\text{II})$  **2b**,  $\text{Ni}(\text{II})$  **2c**,  $[\text{Co}_3\text{X}_6(\text{L1})_2] \cdot n(\text{DMF})$   $\text{X} = \text{Cl}$  **3a**,  $\text{Br}$  **3b** and  $[\text{Co}_3\text{I}_{1.5}(\text{H}_2\text{O})_{4.5}(\text{L1})_2] \cdot 4.5\text{I} \cdot m(\text{DMF})$  **4** were obtained, although crystals of **2c** were of poor quality and only unit cell parameters are presented (see ESI). All structures were determined in the monoclinic space group  $\text{C}2/c$  from X-ray data collected either in-house or using synchrotron radiation. All have an asymmetric unit with one complete L1 ligand, two  $\text{M}(\text{II})$  sites with one on a 2-fold rotation axis, and three terminal

ligands sites. For coordination polymers with nitrate counter-anions (**2a-c**) the nitrates are non-coordinating and terminal ligands on the metal are aquo ligands. Positions of nitrate counter-anions are disordered and could not be located in the difference map. Coordination polymers with halide counter-anions gave essentially the same structure but with halides rather than water adopting the terminal ligand positions where  $\text{X} = \text{Cl}$  (**3a**) and  $\text{Br}$  (**3b**). For compound **4** with iodide counter-anions there is a disorder of the  $\text{I}^-$  positions between terminal ligand positions and uncomplexed lattice positions, Fig. S31, ESI. The  $\text{Co}(\text{II})$  compounds **2a** and **3b** will be used as exemplars and described in more detail.

In all of these coordination polymers the L1 ligand has all isonicotinoyl groups oriented differently and with carbonyl groups *exo* to the L1 molecular cavity, unlike in **1** where they were all oriented inwards. As for **1**,  $\text{M}_6\text{L}_2$  capsule motifs are formed from two head-to-head L1 ligands coordinating to an approximately hexagonal equator of six metal cations, Fig. 5. In **2a** for example, the  $\text{Co} \cdots \text{Co}$  distances around the hexagon range from 9.99 to 10.08 Å, whereas for **3b** they are 10.20 to 10.49 Å, in all cases slightly longer than the equivalent  $\text{Re} \cdots \text{Re}$  distances in **1**. The metal geometry is distorted octahedral with *trans* terminal ligands ( $\text{Co} \cdots \text{OH}_2$  range 2.0559(17) to 2.129(3) Å for **2a**,  $\text{Co} \cdots \text{Br}$  range 2.5955(8) to 2.6045(11) for **3b**) and four isonicotinoyl donors from four symmetry-related L1 ligands ( $\text{Co} \cdots \text{N}$  range 2.133(5) to 2.158(2) Å for **2a**, 2.140(4) to 2.168(4) Å for **3b**). Two  $\text{M}_6\text{L}_2$  capsules are linked together at each metal centre to give a 6-connected 2D network of **hxl** topology as before.

While the 2D coordination polymer network of compound **1** and the isostructural series **2-4** are topologically the same and structurally very similar, the network packing observed for these materials is quite distinct to that of **1**. Adjacent networks viewed from above are positioned such that the triangular gaps within the networks are approximately aligned to form channels through the lattice, Fig. 6a. There are also rectangular channels evident when networks are viewed from the side, Fig. 6b, which are clearly much larger than any spaces between networks

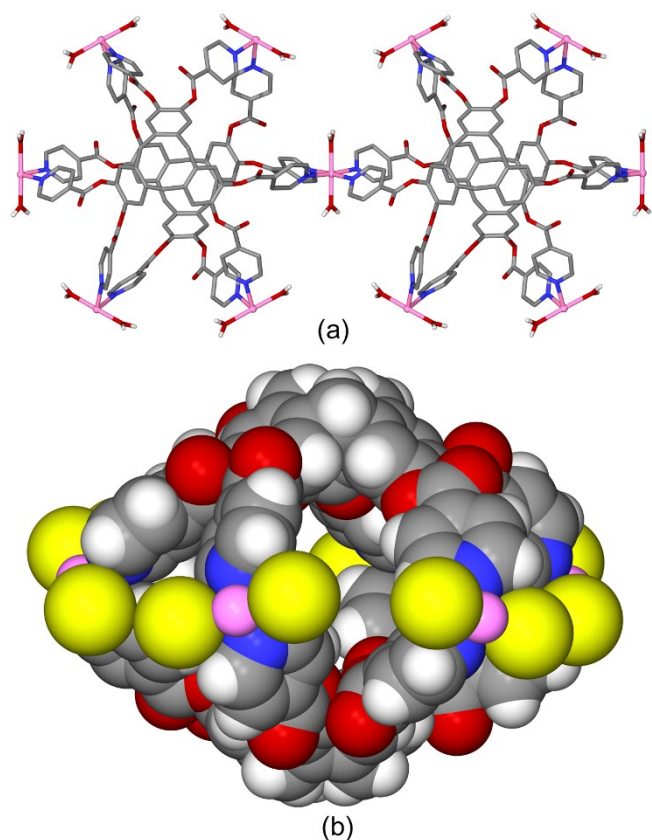


**Fig 5.** From the crystal structures of connected  $M_2L_2$  cage coordination polymer series (a) two connected cages of  $[Co_2(H_2O)_2(L1)_2] \cdot 6(NO_3) \cdot n(DMF)$  **2a** with hydrogens aside from those of aquo ligands excluded; (b) space-filling view of a single cage from  $[Co_2Br_6(L1)_2] \cdot n(DMF)$  **3b**.

observed from a similar perspective of **1** (Fig. 3b). The void spaces within **2-4** are much larger than that of **1**. In **2a**, for example, the solvent-accessible void, which will contain both solvent and counter-anion, accounts for ca. 60% of the unit cell volume. The position of one DMF solvent molecule could be established in the structure of **3b**, and resides in the rectangular channels (Fig. S30, ESI). In **4** there is disorder of the anions and the terminal ligands are refined as 25% I and 75% aquo. Co-O/I bond lengths are in the range 2.349(6) to 2.383(7) Å, much longer than the Co-OH<sub>2</sub> bond lengths seen in **2a** but shorter than anticipated for Co-I. The remaining I is present as lattice I<sup>-</sup> counter-anions which were also disordered and refined at low occupancy, though not all positions were located, Fig. 6c.

The channels in the structures will be occupied by solvent DMF and, where applicable, counter-anions. TGA shows the nitrate compounds (**2a-c**) decompose at lower temperatures than the halide compounds the latter being thermally stable to ca. 350 °C, Figs S17-S21 SI. Using **2a** and **3b** as examples, solvation levels can be estimated from TGA. Compound **2a** has an initial weight loss of ca. 30% weight to ca. 150 °C. This is consistent with the loss of coordinated water ligands plus 14 DMF molecules per formula unit. TGA of **3b** gives a slightly higher mass loss of ca. 35 % corresponding to 19 DMF per formula unit. This is consistent with the probable solvation level calculated on the basis of void calculations.

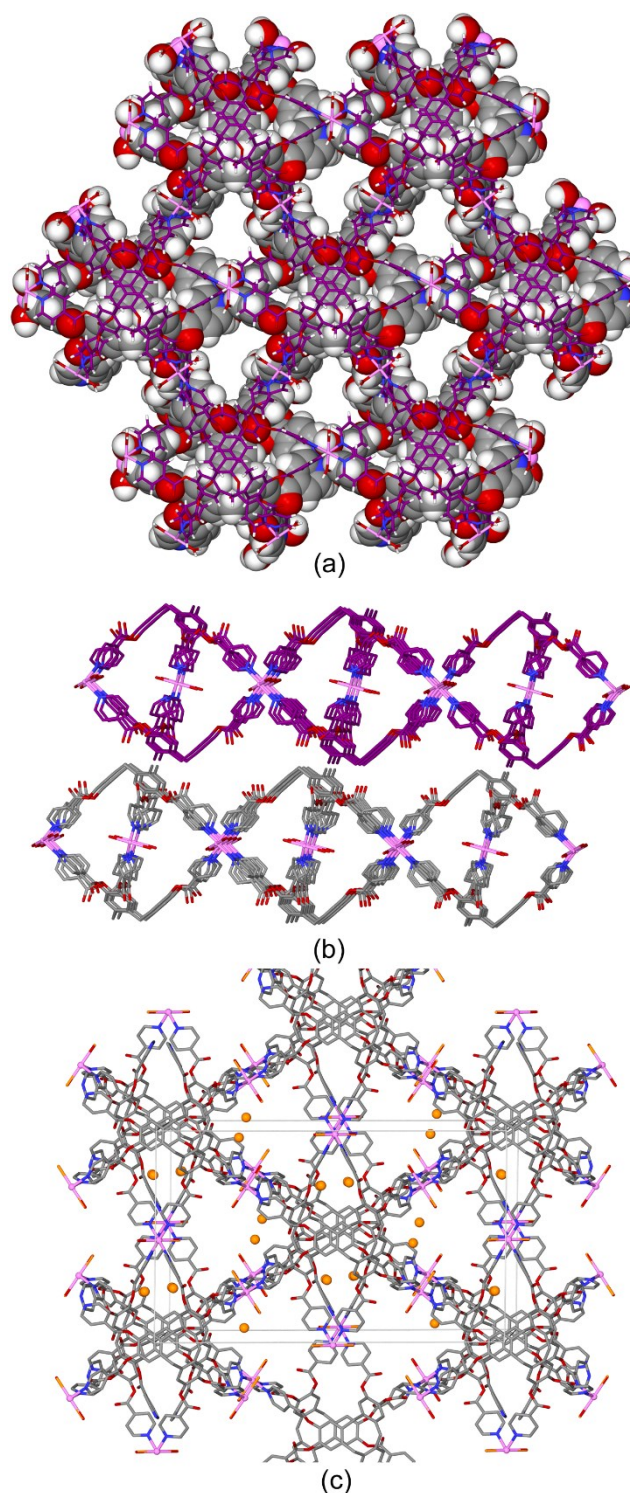


**Fig. 6** Extended packing diagrams of **2a** (a) and (b) highlighting channels within the crystal packing, and (c) unit cell of  $[Co_{3.5}(H_2O)_{4.5}(L1)_2] \cdot 4.5I \cdot m(DMF)$  **4** viewed down *c* with disordered H<sub>2</sub>O/I terminal ligands and lattice I<sup>-</sup> positions (orange spheres).

#### Other Coordination Polymers with L1

While reaction of L1 with  $Cu(NO_3)_2$  gave the **hxl** structure, use of the trifluoroacetate,  $TFA = CF_3CO_2^-$ , salt of Cu(II) led to the isolation of compound  $[Cu_2(L1)(TFA)_3(isonic)] \cdot n(DMF)$  **5** where isonic = iso-nicotinate. Formation of this compound was

repeatable and the isonicotinate is likely to be from some Cu(II)-catalysed decomposition of the ligand. The crystal structure of **5** was determined in space group  $P\bar{1}$  with an asymmetric unit of two Cu(II) centres, one L1 ligand, three TFA anions and one isonic anion. The two Cu(II) centres have different square pyramidal coordination environments, Fig. 7. Cu1 is coordinated by isonicotinoyl groups from three symmetry-related L1 ligands arranged in a T-shape at Cu-N distances 1.977(10) to 2.241(10) Å, alongside one terminal TFA anion (Cu-O 2.033(9) Å), and the carboxylate of a bridging isonic anion (Cu-O 1.949(8) Å). Cu2 also has three pyridyl donors in a T-shape but two are from L1 ligands and the other the isonic anion (Cu-N distances 2.006(11) to 2.210(10) Å). The Cu2 coordination sphere is completed by two terminal TFA ligands at Cu-O distances 1.947(9) and 1.984(8) Å.

The structure of  $[\text{Cu}_2(\text{L1})(\text{TFA})_3(\text{isonic})]$  is a (3,4,5)-connected 2D coordination polymer where each Cu1 is a 4-connecting centre and each Cu2 is a 3-connecting centre. The orientations of the six isonicotinoyl groups of L1 are all distinct, and only five of the six isonicotinoyl groups binds to a Cu(II) cation, making the L1 ligand a 5-connecting centre. Overall a two-tiered 2D network is formed with L1 molecular bowls facing inwards, Fig. 8a. The network is easiest to understand by first considering just the Cu(II)-L1 connectivity, which forms a ladder-motif with two layers of L1 ligands with the non-coordinating isonicotinoyl group directed outwards, Fig. 8b. The orientation of L1 bowls in the ladder alternates for each layer, and the Cu2 sites are at the edges of the ladder, and two layers of Cu1 centres in the middle. Within the 2D network, these Cu(II)-L1 ladders are linked together via the bridging isonic anion which bridges between Cu1 and Cu2 centres, shown for two ladder motifs only in Fig. 8b. This gives an extended capsule-like motif between L1 ligands of opposite orientation from adjacent ladders. These inter-ladder connections extend out into the 2D network.

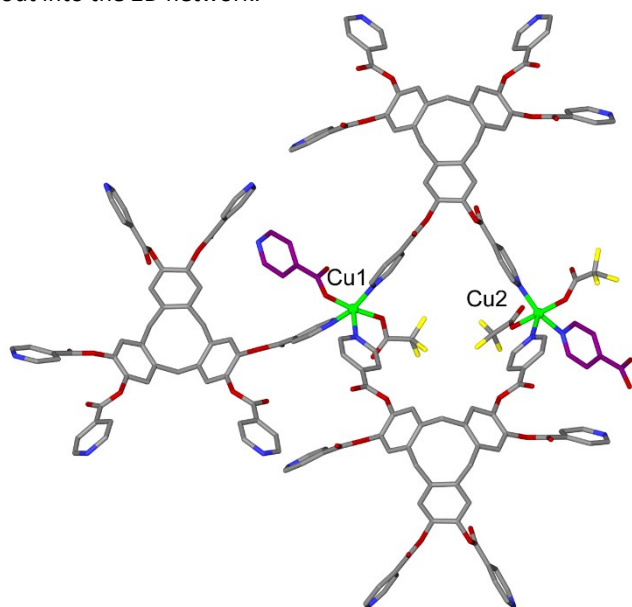


**Fig. 7** From the crystal structure of  $[\text{Cu}_2(\text{L1})(\text{TFA})_3(\text{isonic})] \cdot n(\text{DMF})$  **5** highlighting two different Cu(II) coordination environments and with isonic anion in purple

The  $[\text{Cu}_2(\text{L1})(\text{TFA})_3(\text{isonic})]$  coordination polymers stack together to give the crystal lattice shown in Fig. 9. There are significant solvent-accessible voids running through the lattice, estimated at ca. 50% of the unit cell volume. These are likely to be occupied by solvent DMF although this was not located in the crystal structure. TGA indicates a weight loss of ca. 30 % to 200 °C after which the material decomposes, Fig. S21. This corresponds to 10 DMF molecules per formula unit which can easily be accommodated within this void space.

The crystalline material  $[\text{Ag}_2(\text{L1})(\text{DMF})_2] \cdot 2\text{BF}_4 \cdot 2(\text{H}_2\text{O}) \cdot 6(\text{DMF})$  **6** is isolated from vapor

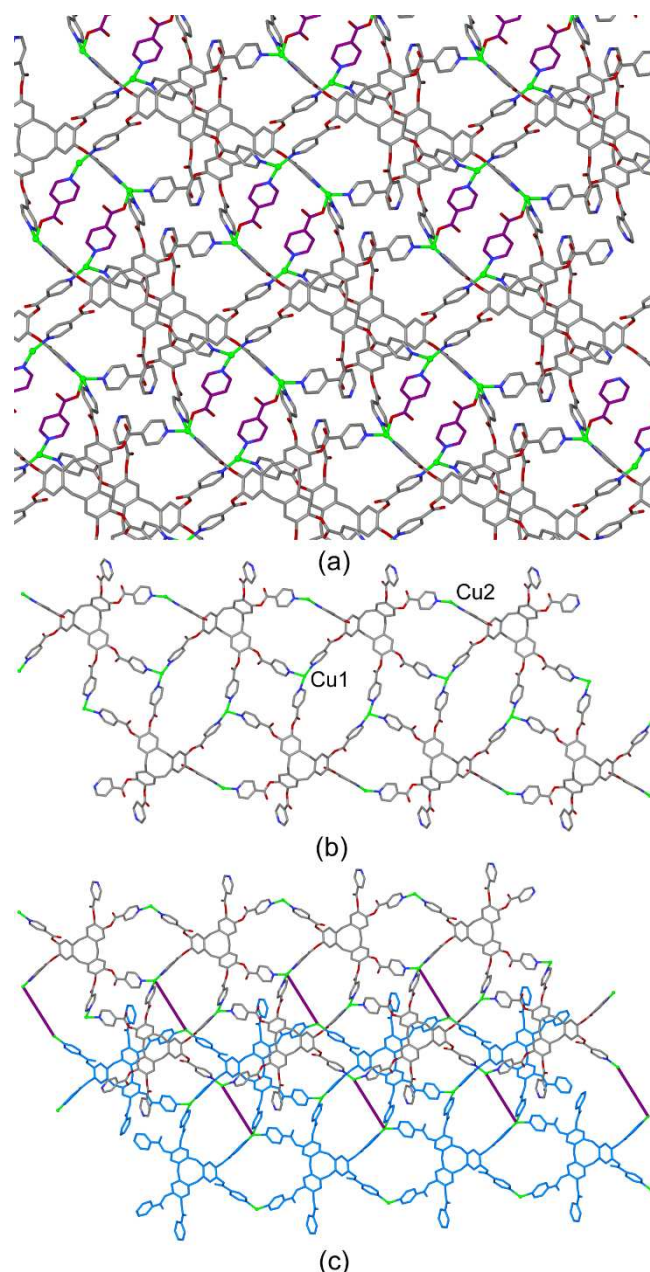


**Fig. 8** From the crystal structure of **5** (a) 2D coordination polymer network with TFA anions excluded and isonic anion shown in purple; (b) breakdown of the network with (top) bridging isonicotinate anion excluded giving a Cu1 ladder motif, and (bottom) connectivity of two such ladders through bridging isonic anion shown as purple line for clarity.

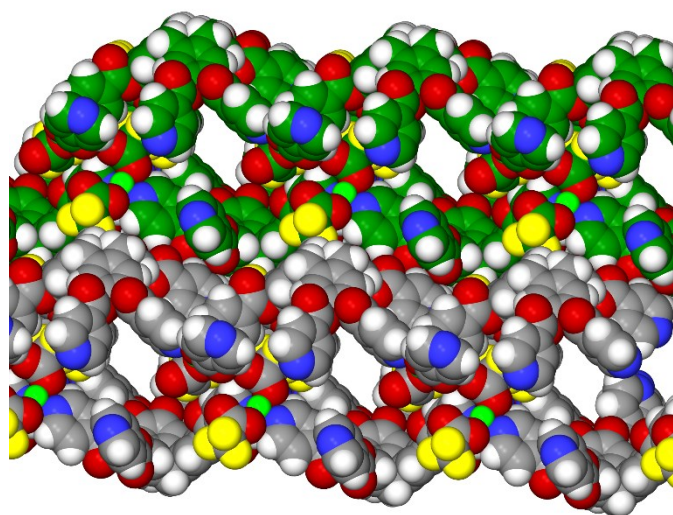


**Fig. 9** Packing diagram of **5** viewed down *a* unit cell in space-filling mode with two 2D polymers in different colours.

diffusion of diethylether into a DMF solution of  $\text{AgBF}_4$  and L1. The single crystal X-ray structure was determined in monoclinic space group  $P2_1/m$ . The asymmetric unit comprises one  $\text{Ag(I)}$ , half of an L1 ligand,  $\text{BF}_4^-$  counter-anion and solvent molecules. The L1 ligand has mirror symmetry. The  $\text{Ag(I)}$  is coordinated by a terminal DMF at  $\text{Ag-O}$  distance 2.553(4) Å, and three pyridyl groups from three symmetry-related L1 ligands at  $\text{Ag-N}$  distances 2.231(3) to 2.348(4) Å. The coordination geometry is distorted trigonal pyramidal rather than tetrahedral with the DMF in the apical position. The  $\text{Ag(N)}_3$  atoms are near coplanar with  $\text{N-Ag-N}$  angles 103.35(14), 121.13(15) and 135.23(14)°. Each L1 bridges to six  $\text{Ag(I)}$  positions and an undulating 2D coordination polymer is formed. The network is of (3,6)-connectivity and has a kagome dual (**kgd**) topology, Fig. 10.<sup>22</sup> Examples of coordination polymers with the kagome dual topology are relatively uncommon<sup>30</sup> although  $\text{ML}_2$  examples with tripodal CTV-type ligands have been reported.<sup>14c</sup> Here the  $\text{M}_2\text{L}$  stoichiometry has a six-connected ligand centre rather than the six-connected metal of the  $\text{ML}_2$  example. The 2D polymer has a wave-like aspect when viewed side-on due to the orientation of the L1 ligand (bowl-up or bowl-down) alternating along the *b* axis. A solvent DMF molecule occupies each L1 bowl with a methyl group oriented towards the hydrophobic bowl. Packing of the  $[\text{Ag}_2(\text{L1})(\text{DMF})_2]^+$  networks creates lattice sites which are occupied by additional DMF, water and  $\text{BF}_4^-$  counter-anions, Fig. S33.

## Experimental

### Synthetic procedures

Cyclotricatechylene (CTC)<sup>35</sup> and  $\text{Re}(\text{CO})_5\text{Br}$ <sup>36</sup> were synthesised by literature methods. Other chemicals were obtained from commercial sources and used as received. NMR spectra were recorded on a Bruker DPX 300 MHz NMR spectrometer. ESI-MS were measured on a Bruker Maxis Impact instrument in positive

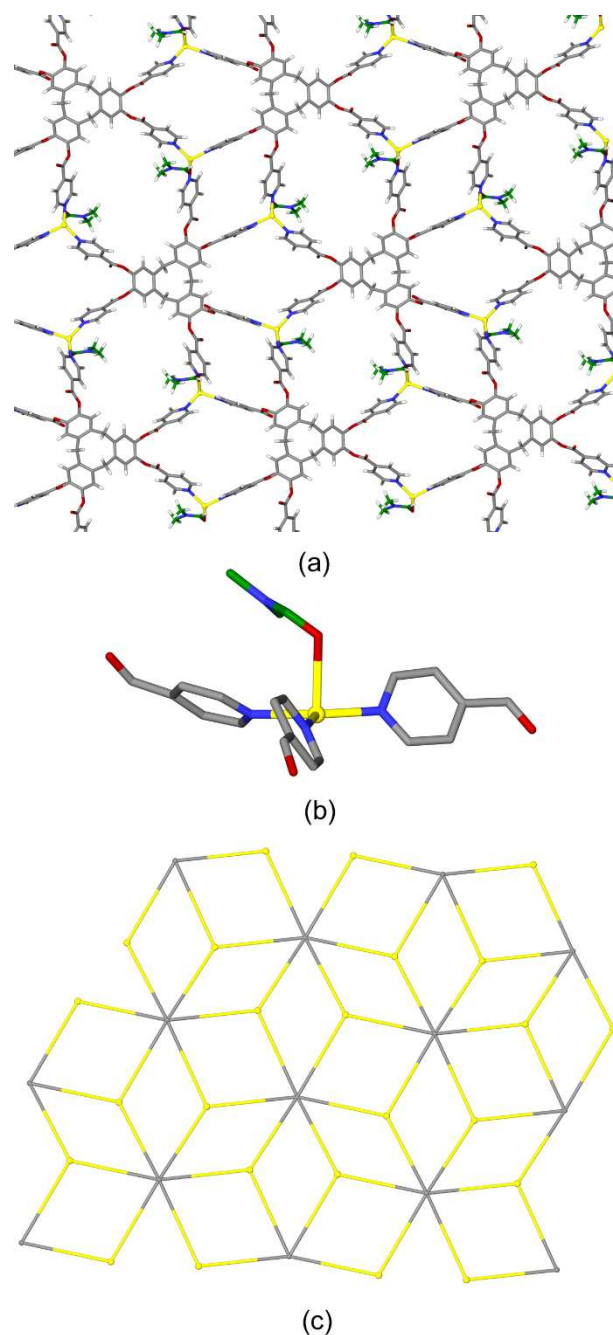


**Fig. 10** From the crystal structure of  $[\text{Ag}_2(\text{L1})(\text{DMF})_2] \cdot 2\text{BF}_4 \cdot 2(\text{H}_2\text{O}) \cdot 6(\text{DMF})$  **6**. (a)  $[\text{Ag}_2(\text{L1})(\text{DMF})_2]^+$  2D coordination polymer; (b) highlight of coordination environment of  $\text{Ag(I)}$ ; (c) connectivity diagram showing kagome dual topology with large spheres  $\text{Ag(I)}$  and small spheres the centroid of coordinating N-atoms of L1. DMF shown with C in green, Ag as yellow spheres.

ion mode. Infra-red spectra were recorded as solid phase samples on a Bruker ALPHA Platinum ATR. Elemental analyses were performed by the service at the London Metropolitan University.

### (±)-2,3,7,8,12,13-Hexa(pyridyl-4-carboxylate)-10,15-dihydro-5H-tribenzo[*a,d,g*]cyclononene

**(hexakis(isonicotinoyl)cyclotricatechylene L1)** CTC (0.4 g, 1.09 mmol) and triethylamine (24 ml) were added to dry tetrahydrofuran (250 ml) under  $\text{N}_2$  atmosphere. The reaction was cooled in ice for 1 hour. Isonicotinoyl chloride



hydrochloride (2.34 g, 13.15 mmol) was added to the reaction to give a suspension that was stirred at room temperature for two days. Solvent was removed under vacuum, and methanol (ca. 20 ml) was added to the residue. The mixture was sonicated and solid collected by filtration, washed with methanol and diethyl ether to give L1 as white solid (0.71 g, 0.71 mmol, 65 %).  $^1\text{H}$  NMR (300 MHz,  $d_6$ -DMSO)  $\delta$  (ppm) 8.76 (d,  $J = 5.0$  Hz, 4H,  $H_{\text{py\_ortho}}$ ), 7.88 – 7.78 (m, 6H,  $H_{\text{arene}} + H_{\text{py\_meta}}$ ), 5.17 (d,  $J = 13.9$  Hz, 1H,  $\text{CH}_2\text{-exo}$ ), 3.95 (d,  $J = 13.6$  Hz, 1H,  $H_{2\text{-endo}}$ ).  $^{13}\text{C}$  NMR (75 MHz,  $d_6$ -DMSO)  $\delta$  (ppm) 162.53, 151.02, 140.15, 138.76, 135.13, 125.05, 122.62, 34.99. HR MS (ES+):  $m/z$  997.2758  $\{M+H\}^+$  (calc. 997.2469), 499.1406  $\{M+2H\}^{2+}$ , 333.0961  $\{M+3H\}^{3+}$ . FT IR:  $\nu$  ( $\text{cm}^{-1}$ ) 1753.05 (sharp, C=O ester stretch), 1597.08, 1562.38 (medium, C=C stretch), 1504.48, 1448.15 (medium, C-C in-ring aromatic stretch), 1484.08, 1252.02 (sharp, C-N aromatic amine stretch), 1132.72 (sharp, C-O ester stretch). M.pt 297–299°C. Elemental analysis (%) for L1·3H<sub>2</sub>O calc C 65.13, H 4.03, N 8.00; obs C 65.24, H 3.93, N 7.84.

**[Re<sub>3</sub>(L1)<sub>2</sub>Br<sub>3</sub>(CO)<sub>3</sub>] $\cdot$ n(MeNO<sub>2</sub>) $\cdot$ m(H<sub>2</sub>O) 1** L1 (20 mg, 0.020 mmol) and Re(CO)<sub>5</sub>Br (0.030 mmol) were dissolved in nitromethane (4 ml) and the mixture was heated to give a bright yellow solution. The sealed reaction vessel was heated at 60 °C using a heating block for two days. Pale yellow crystals form on cooling. Selected FT-IR  $\nu$  ( $\text{cm}^{-1}$ ) **1** 3060.18, 2020.81 (C=O), 1874.35, 1749.88 (C=O), 1659.40, 1385.63, 1326.44, 1257.4, 1087.36. Elemental analysis indicates high solvation levels as expected for material with ca. 1200 Å<sup>3</sup> void space per formula unit (%) calc for [Re<sub>3</sub>(L1)<sub>2</sub>Br<sub>3</sub>(CO)<sub>3</sub>] $\cdot$ 7(MeNO<sub>2</sub>) $\cdot$ 10(H<sub>2</sub>O) C 42.73, H 3.27, N 7.64; found C 40.85, H 2.17, N 4.76.

#### General method for formation of coordination polymer materials 2a – 5

Ligand L1 (10 mg) and appropriate metal salt (M(NO<sub>3</sub>)<sub>2</sub> $\cdot$ n(H<sub>2</sub>O), CoCl<sub>2</sub>, CoBr<sub>2</sub>, CoI<sub>2</sub> or Co(CF<sub>3</sub>CO<sub>2</sub>)<sub>2</sub> 5 mg) were dissolved in DMF (2 ml) in a small sample vial which was capped and a hole punched in the cap. This was placed in a larger vial containing diethyl ether which was capped and left to stand. Crystals grow after several days or weeks. Single crystals grow with a small amount of amorphous powdered material and it is difficult to fully separate the two. This and the high and unknown solvation levels of materials mean it was difficult to obtain satisfactory or meaningful elemental analysis results. Full CHN analyses, and IR data is given for all compounds in the Supplementary Material. Sample data for compound **4**: Selected FT-IR  $\nu$  ( $\text{cm}^{-1}$ ) 3437.42, 2927.21, 1748.31, 1653.30, 1597.31, 1504.08, 1437.18, 1407.33, 1251.98, 1175.20, 1086.68, 1059.63. Elemental analysis (%) calc for Co<sub>3</sub>I<sub>2</sub>(L1)<sub>2</sub> $\cdot$ 10(H<sub>2</sub>O) $\cdot$ 2(DMF) C 44.21, H 3.28 N 6.02; found C 43.75, H 3.74, N 7.02.

**[Ag<sub>2</sub>(L1)(DMF)<sub>2</sub>] $\cdot$ 2BF<sub>4</sub> $\cdot$ 2(H<sub>2</sub>O) $\cdot$ 6(DMF) 6** Ligand L1 (10 mg, 0.01 mmol) was dissolved in DMF (1.5 ml) and added to a solution of AgBF<sub>4</sub> (2.3 mg, 0.015 mmol) in DMF (0.5 ml). Vapors of diethyl ether were allowed to diffuse into the solution to give colourless block-like crystals. Selected FT-IR  $\nu$  ( $\text{cm}^{-1}$ ) 3113.17, 2929.80, 1748.47 (C=O), 1651.00, 1494.97, 1420.54, 1389.92, 1255.91, 1055.93. Elemental analysis (%) for [Ag<sub>2</sub>(L1)(DMF)<sub>2</sub>] $\cdot$ 2BF<sub>4</sub> $\cdot$ 4(H<sub>2</sub>O) $\cdot$ 6(DMF) calc. C 47.59, H 4.93, N 9.60; found C 47.62, H 4.95, N 11.88.

#### X-Ray Crystallography

Crystals were mounted under inert oil on a MiTeGen tip and flash frozen to 100(1) or 120(1) K. X-ray diffraction data were collected using Cu-K $\alpha$  radiation ( $\lambda = 1.54184$  Å) using an Agilent Supernova dual-source diffractometer with Atlas S2 CCD detector and micro-focus sealed tube generator, or using synchrotron radiation ( $\lambda = 0.6889$  Å) at station I19 of Diamond Light Source. Data were corrected for Lorentzian and polarization effects and absorption corrections were applied using multi-scan methods. The structures were solved by direct methods using SHELXS,<sup>37</sup> or charge flipping using SUPERFLIP,<sup>38</sup> and refined by full-matrix least squares on  $F^2$  using SHELXL.<sup>37</sup> Unless otherwise specified, all non-hydrogen atoms were refined as anisotropic, and hydrogen positions were included at geometrically estimated positions. Most materials were weakly diffracting and did not diffract to high angles. Uncomplexed counter-anions were generally not located but were included in the formula. The structures of compounds **2a**, **2b**, **3a**, **3b**, **4** and **5** showed significant void space with residual electron density which could not be meaningfully refined as solvent molecules and/or counter-anions. Thus the data for these materials was treated with the SQUEEZE procedure of PLATON.<sup>39</sup> Additional details of data collections and structure are given below and in Table 1.

In compound **1** the solvent atoms were refined isotropically and global restraints were used on anisotropic displacement parameters, water positions are disordered and modelled at part occupancy. Compound **3b** was refined with one N-C bond length of a DMF restrained to be chemically reasonable, and DMF refined isotropically. For **4** not all lattice disordered I<sup>-</sup> positions were located in the difference map. Disordered aquo/I ligands and lattice I<sup>-</sup> were refined isotropically. Disordered aquo/I ligands were modelled as 0.75:0.25 O:I. For [Cu<sub>2</sub>(L1)(TFA)<sub>3</sub>(isonic)] **5** only Cu positions were refined anisotropically due to weak data. Two trifluoroacetate anions were treated with restraints on some bond lengths and one CO<sub>2</sub><sup>-</sup> group restrained to be flat. Compound **6** disordered water was refined isotropically.

Table 1: Details of X-ray data collections and structure refinements.

	L1-DMF*	1	2a	2b	3a
CCDC	1823167	1823166	1823168	1823169	1823170
Formula	C <sub>60</sub> H <sub>43</sub> N <sub>7</sub> O <sub>13</sub>	C <sub>119</sub> H <sub>90</sub> Br <sub>3</sub> N <sub>14</sub> O <sub>37</sub> Re <sub>3</sub>	C <sub>114</sub> H <sub>84</sub> Co <sub>3</sub> N <sub>18</sub> O <sub>48</sub>	C <sub>114</sub> H <sub>84</sub> Cu <sub>3</sub> N <sub>18</sub> O <sub>48</sub>	C <sub>114</sub> H <sub>72</sub> Cl <sub>6</sub> Co <sub>3</sub> N <sub>12</sub> O <sub>24</sub>
<i>Mr</i>	1070.01	3106.38	2650.78	2664.61	2383.33
Crystal colour	Colourless	Yellow	Orange	Pale blue	Pink
Crystal size (mm)	0.12 x 0.10 x 0.07	0.20 x 0.19 x 0.15	0.08 x 0.08 x 0.03	0.24 x 0.14 x 0.08	0.10 x 0.06 x 0.03
Crystal system	Triclinic	Trigonal	Monoclinic	Monoclinic	Monoclinic
Space group	$P\bar{1}$	$R\bar{3}m$	$C2/c$	$C2/c$	$C2/c$
<i>a</i> (Å)	13.6325(4)	19.6665(4)	34.7067(11)	34.8581(12)	35.226(3)
<i>b</i> (Å)	14.2524(2)	19.6665(4)	20.1430(5)	20.3238(7)	20.1867(12)
<i>c</i> (Å)	14.6263(6)	31.6873(10)	32.4896(13)	30.9326(9)	33.622(2)
$\alpha$ (°)	81.277(3)	90	90	90	90
$\beta$ (°)	67.960(3)	90	103.879(4)	97.984(3)	110.454(9)
$\gamma$ (°)	79.096(2)	120	90	90	90
<i>V</i> (Å <sup>3</sup> )	2576.42(13)	10613.8(5)	22050.3(13)	21701.8(12)	22401(3)
<i>Z</i>	2	3	4	4	4
$\rho_{\text{calc}}$ (g.cm <sup>-3</sup> )	1.379	1.458	0.798	0.816	0.707
$\vartheta$ range (°)	1.46–36.20	2.95–73.56	4.02–51.33	2.89–74.21	3.13–55.0
No. data collected	56317	7896	26709	40034	70212
No. unique data	23748	2571	11837	19201	14078
<i>R</i> <sub>int</sub>	0.046	0.0384	0.0346	0.0467	0.1669
No. obs. Data ( <i>I</i> > 2σ( <i>I</i> ))	13103	2444	7782	7247	7635
No. parameters	723	128	644	717	717
No. restraints	0	113	0	0	0
<i>R</i> <sub>1</sub> (obs data)	0.0642	0.1496	0.0841	0.0957	0.1297
<i>wR</i> <sub>2</sub> (all data)	0.2075	0.5003	0.2882	0.3043	0.3663
<i>S</i>	0.969	2.482	1.107	0.999	1.080
	<b>3b*</b>	<b>4</b>	<b>5</b>	<b>6</b>	
CCDC	1823171	1823172	1823165	1823164	
Formula	C <sub>120</sub> H <sub>86</sub> Br <sub>6</sub> Co <sub>3</sub> N <sub>14</sub> O <sub>26</sub>	C <sub>114</sub> H <sub>81</sub> Co <sub>3</sub> I <sub>6</sub> N <sub>12</sub> O <sub>28.5</sub>	C <sub>69</sub> H <sub>40</sub> Cu <sub>2</sub> F <sub>9</sub> N <sub>7</sub> O <sub>20</sub>	C <sub>81</sub> H <sub>96</sub> Ag <sub>2</sub> B <sub>2</sub> F <sub>8</sub> N <sub>14</sub> O <sub>22</sub>	
<i>Mr</i>	2796.28	3013.10	1585.16	2007.08	
Crystal colour	Pale pink	Orange	Blue	Colourless	
Crystal size (mm)	0.13 x 0.12 x 0.06	0.05 x 0.05 x 0.04	0.07 x 0.04 x 0.03	0.10 x 0.04 x 0.01	
Crystal system	Monoclinic	Monoclinic	Triclinic	Monoclinic	
Space group	$C2/c$	$C2/c$	$P\bar{1}$	$P2_1/m$	
<i>a</i> (Å)	35.9310(11)	35.4694(8)	18.1806(11)	11.8036(1)	
<i>b</i> (Å)	20.5186(5)	20.3503(5)	18.4809(11)	33.2827(4)	
<i>c</i> (Å)	32.4986(15)	33.3657(7)	19.4599(13)	12.5383(1)	
$\alpha$ (°)	90	90	103.319(6)	90	
$\beta$ (°)	111.330(3)	110.579(3)	109.243(6)	109.616(1)	
$\gamma$ (°)	90	90	103.091(5)	90	
<i>V</i> (Å <sup>3</sup> )	22318.5(14)	22547.0(9)	5672.3(7)	4639.87(8)	
<i>Z</i>	4	4	2	2	
$\rho_{\text{calc}}$ (g.cm <sup>-3</sup> )	0.832	0.888	0.928	1.437	
$\vartheta$ range (°)	1.13–25.17	2.83–59.64	2.978–51.417	3.97–73.88	
No. data collected	79562	19206	27829	20679	
No. unique data	21159	13349	11988	9253	
<i>R</i> <sub>int</sub>	0.0402	0.0344	0.0778	0.0374	
No. obs. Data ( <i>I</i> > 2σ( <i>I</i> ))	12776	9188	6609	8333	
No. parameters	735	715	439	602	
No. restraints	1	0	4	0	
<i>R</i> <sub>1</sub> (obs data)	0.0884	0.1409	0.1249	0.0704	
<i>wR</i> <sub>2</sub> (all data)	0.3030	0.4171	0.3868	0.2009	
<i>S</i>	1.060	1.559	1.055	1.036	

\* data collected using synchrotron radiation ( $\lambda = 0.6889 \text{ \AA}$ )

## Conclusions

The hexapodal ligand *tris*(isonicotinoyl)cyclotriguaiacyclene has been successfully synthesised and forms a series of coordination polymers with transition metals with a predominance of 2D networks of linked  $M_6L_2$ -cage structures. The relative lack of conformational flexibility of the ester linker group which attached the metal-binding pyridyl groups and bowl-shaped host scaffold mean that the ligand reliably acts as a hexagonal-linker affording the relatively rare network topologies **hxl** and **kgd**. There are two types of analogous cage-linked coordination polymer, the high-symmetry structure with Re(I) and lower symmetry versions with other transition metals. These show different stacking patterns between 2D their layers, both with channels throughout the structure and the materials show stability to solvent loss. The formation of metallo-cage motifs within a coordination polymer ensures that the molecular binding site of the host-type ligand is not blocked by self-inclusion, and coordination polymer **1** has been shown to uptake the neutral molecular guest  $I_2$  from solution.

## Conflicts of interest

There are no conflicts to declare.

## Acknowledgements

We thank The Leverhulme Trust (RPG-2014-148) and the University of Leeds for funding and the EPSRC for equipment funding (EP/K039202/1). This work was carried out with support from the Diamond Light Source (MT-10344). We thank Christopher Sumby for assistance with synthesis, Stephen Boyer for microanalyses, and Algy Kazlaucinas for SEM-EDX measurements.

## Notes and references

‡ **Data Accessibility** Data supporting this study are available at <https://doi.org/10.5518/399>

- J. J. Perry, J. A. Perman and M. J. Zaworotko, *Chem. Soc. Rev.*, 2009, **38**, 1400; S. Noro, S. Kitagawa, T. Akutagawa and T. Nakamura, *Prog. Polym. Sci.*, 2009, **34**, 240; A. Y. Robin and K. M. Fromm, *Coord. Chem. Rev.*, 2006, **250**, 2127; N. W. Ockwig, O. Delgado-Friedrichs, M. O'Keeffe, O. M. Yaghi, *Acc. Chem. Res.*, 2005, **38**, 176; C. Janiak, *Dalton Trans.*, 2003, 2781; S. L. James, *Chem. Soc. Rev.*, 2003, **32**, 276; R. Robson, *J. Chem. Soc., Dalton Trans.*, 2000, 3735.
- recent reviews C. H. Hendon, A. J. Rieth, A. J.; Korzyński and M. Dincă, *ACS Central Sci.*, 2017, **3**, 554; C.-D. Wu and M. Zhao, *Adv. Mater.*, 2017, **29**, 1605446; C. A. Trickett, A. Helal, B. A. Al-Maythalyony, Z. H. Yamani, K. E. Cordova and O. M. Yaghi, *Nature Rev. Mater.*, 2017, **2**, 17045; S. M. Cohen, Z. Zhang and J. A. Boissonnault, *Inorg. Chem.*, 2016, **55**, 7281; Z. R. Herm, E. D. Bloch and J. R. Long, *Chem. Mater.*, 2014, **26**, 323; P. Horcajada, R. Gref, T. Baati, P. K. Allan, G. Maurin, P. Couvreur, G. Férey, R. E. Morris, C. Serre, *Chem. Rev.*, 2012, **112**, 1232; S. T. Meek, J. A. Greathouse and M. D. Allendorf, *Adv. Mater.*, 2011, **23**, 249.
- for example H. Zhang, R. Zou and Y. Zhao, *Coord. Chem. Rev.*, 2015, **292**, 74; W. J. Gee, B. Moubaraki, K. S. Murray and S. R. Batten, *CrystEngComm*, 2013, **15**, 9655; J. J. Gassensmith, H. Furukawa, R. A. Smaldone, R. S. Forgan, Y. Y. Botros, O. M. Yaghi, and J. F. Stoddart, *J. Am. Chem. Soc.*, 2011, **133**, 15312; P. Thuery, *Cryst. Growth Des.*, 2009, **9**, 1208.
- for example J. Aguilera-Sigalat, C. Sáenz de Pipaón, D. Hernández-Alonso, E. C. Escudero-Adán, J. R. Galan-Mascaró and P. A. Ballester, *Cryst. Growth Des.*, 2017, **17**, 1328; R. Pinalli, E. Dalcanale, F. Ugozzoli and C. Massera, *CrystEngComm*, 2016, **18**, 5788; S. P. Bew, A. D. Burrows, T. Düren, M. F. Mahon, P. Z. Moghadam, V. M. Sebestyen and S. Thurston, *Chem. Commun.*, 2012, **48**, 4824; E. J. Kim, J. Ahn, H. Lee, T. H. Noh and O.-S. Jung, *Tetrahedron Lett.*, 2012, **53**, 1240; S. Tashiro, S. Hashida and M. A. Shionoya, *Chem. Asian J.*, 2012, **7**, 1180; M. W. Hosseini, *Acc. Chem. Res.*, 2005, **38**, 313; M. Tadokoro, S. Mizugaki, M. Kozaki and K. Okada, *Chem. Commun.*, 2005, 1140; S. J. Dalgarno and C. L. Raston, *Chem. Commun.*, 2002, 2216.
- P. P. Cholewa, C. M. Beavers, S. J. Teat, S. J. Dalgarno, *Cryst. Growth Des.*, 2013, **13**, 5165.
- H. Tan, S. Du, Y. Bi and W. Liao, *Chem. Commun.*, 2013, **49**, 8211.
- Y.-J. Hu, J. Yang, Y.-Y. Liu, S. Song and J.-F. Ma, *Cryst. Growth Des.*, 2015, **15**, 3822.
- A. V. Mossine, C. M. Mayhan, D. A. Fowler, S. J. Teat, C. A. Deakynne and J. L. Atwood, *Chem. Sci.*, 2014, **5**, 2297.
- D. A. Fowler, A. V. Mossine, C. M. Beavers, S. J. Teat, S. J. Dalgarno and J. L. Atwood, *J. Am. Chem. Soc.*, 2011, **133**, 11069.
- F. L. Thorp-Greenwood, T. K. Ronson and M. J. Hardie, *Chem. Sci.*, 2015, **6**, 5779.
- T. K. Ronson and M. J. Hardie, *CrystEngComm*, 2008, **10**, 1731.
- A. D. Martin, T. L. Easun, S. P. Argent, W. Lewis, A. J. Blake and M. Schröder, *CrystEngComm*, 2017, **19**, 603.
- C. Zhang, R. S. Patil, C. Liu, C. L. Barnes and J. L. Atwood, *J. Am. Chem. Soc.*, 2017, **139**, 2920.
- B. F. Abrahams, N. J. FitzGerald and R. Robson, *Angew. Chem., Int. Ed.*, 2010, **49**, 2896.
- J.-T. Yu, J. Sun, Z.-T. Huang and Q.-Y. Zheng, *CrystEngComm*, 2012, **14**, 112.
- J. J. Henkelis, S. A. Barnett, L. P. Harding and M. J. Hardie, *Inorg. Chem.*, 2012, **51**, 10657.
- M. A. Little, T. K. Ronson and M. J. Hardie, *Dalton Trans.*, 2011, **40**, 12217; C. Carruthers, T. K. Ronson, C. J. Sumby, A. Westcott, L. P. Harding, T. J. Prior, P. Rizkallah and M. J. Hardie, *Chem. Eur. J.*, 2008, **14**, 10286.
- J. J. Henkelis and M. J. Hardie, *CrystEngComm*, 2014, **16**, 8138; J. J. Henkelis, T. K. Ronson and M. J. Hardie, *CrystEngComm*, 2014, **16**, 3688; M. A. Little, M. A. Halcrow, L. P. Harding and M. J. Hardie, *Inorg. Chem.*, 2010, **49**, 9486; C. Carruthers, J. Fisher, L. P. Harding and M. J. Hardie, *Dalton Trans.*, 2010, 355; C. J. Sumby, J. Fisher, T. J. Prior and M. J. Hardie, *Chem. Eur. J.*, 2006, **12**, 2945; C. J. Sumby and M. J. Hardie, *Cryst. Growth & Des.*, 2005, **5**, 1321; M. J. Hardie and C. J. Sumby, *Inorg. Chem.*, 2004, **43**, 6872.
- recent reviews M. J. Hardie, *Chem. Lett.*, 2016, **45**, 1336; J. J. Henkelis and M. J. Hardie, *Chem. Commun.*, 2015, **51**, 11929; P. P. Cholewa and S. J. Dalgarno, *CrystEngComm*, 2014, **16**, 3655; R. Pinalli, F. Boccini and E. Dalcanale, *Isr. J. Chem.*, 2011, **51**, 781; P. Jin, S. J. Dalgarno and J. L. Atwood, *Coord. Chem. Rev.*, 2010, **254**, 1760.

- 20 W.-J. Hu, L.-Q. Liu, M.-L. Ma, X.-L. Zhao, Y. A. Liu, X.-Q. Mi, B. Jiang, and K. Wen, *Inorg. Chem.*, 2013, **52**, 9309; S. T. Mough and K. T. Holman, *Chem. Commun.*, 2008, 1407.
- 21 J. J. Loughrey, N. J. Patmore, A. Baldansuren, A. J. Fielding, E. L. McInnes, M. J. Hardie, S. Sproules and M. A. Halcrow, *Chem. Sci.*, 2015, **6**, 6935; B. F. Abrahams, B. A. Boughton, N. J. FitzGerald, J. L. Holmes and R. Robson, *Chem. Commun.*, 2011, **47**, 7404; S. S. Bohle and D. Stasko, *Chem. Commun.*, 1998, 567.
- 22 J. A. Wytko, C. Boudon, J. Weiss and M. Gross, *Inorg. Chem.*, 1996, **35**, 4469.
- 23 C. J. Sumby, K. C. Gordon, T. J. Walsh and M. J. Hardie, *Chem. Eur. J.*, 2008, **14**, 4415.
- 24 M. J. Hardie, R. M. Mills and C. J. Sumby, *Org. Biomol. Chem.*, 2004, **2**, 2958.
- 25 D. Xia, Y. Li, K. Jie, B. Shi and Y. A. Yao, *Org. Lett.*, 2016, **18**, 2910.
- 26 M. O'Keefe, M. A. Peskov, S. J. Ramsden and O. M. Yaghi, *Acc. Chem. Res.*, 2008, **41**, 1782.
- 27 J. Jia, A. J. Blake, N. R. Champness, P. Hubberstey and C. Wilson, *Inorg. Chem.*, 2008, **47**, 8652.
- 28 for example V. Sharma, D. De, S. Pal, P. Saha and P. K. Bharadwaj, *Inorg. Chem.*, 2017, **56**, 8847; H. L. Nguyen, F. Gándara, H. Furukawa, T. J. H. Doan, K. E. Cordova and O. M. Yaghi, *J. Am. Chem. Soc.*, 2016, **138**, 4330; Y.-L. Gai, K.-C. Xiaong, L. Chen, Y. Bu, X.-J. Li, F.-L. Jiang, *Inorg. Chem.*, 2012, **51**, 13128; L. Zhang, F. Liu, Y. Guo, X. Wang, J. Guo, Y. Wei, Z. Chen and D. Sun, *Cryst. Growth Des.*, 2012, **12**, 6215; S. Geranmayeh, A. Abbasi, M. Y. Skripkin and A. Badiei, *Polyhedron*, 2012, **45**, 204; X. Pan, J. Xu, H. Zheng, K. Huang, Y. Li, Z. Guo and S. R. Batten, *Inorg. Chem.*, 2009, **48**, 5772.
- 29 for example, A. V. Ermolaev, A. I. Smolentsev and Y. V. Mironov, *Polyhedron*, 2015, **102**, 417.
- 30 J. Martinex-Lillo, D. Armentano, F. R. Fortea-Perez, S.-E. Stiriba, G. De Munno, F. Lloret, M. Julve and J. A. Faus, *Inorg. Chem.*, 2015, **54**, 4594; T. L. Easun, J. Jia, T. J. Reade, X.-Z. Sun, E. S. Davies, A. J. Blake, M. W. George and N. R. Champness, *Chem. Sci.*, 2014, **5**, 539.
- 31 J. J. Henkelis, C. J. Carruthers, S. E. Chambers, R. Clowes, A. I. Cooper, J. Fisher and M. J. Hardie, *J. Am. Chem. Soc.*, 2014, **136**, 14393.
- 32 D. Shetty, J. Raya, D. S. Han, Z. Asfari, J.-C. Olsen and A. Trabolsi, *Chem. Mater.*, 2017, **29**, 8968; K. Jie, Y. Zhou, E. Li, Z. Li, R. Zhao and F. Huang, *J. Am. Chem. Soc.*, 2017, **139**, 15320; T. Hasell, M. Schmidtman and A. I. Cooper, *J. Am. Chem. Soc.*, 2011, **133**, 14920; T. Hertzsch, F. Budde, E. Weber and J. Hulliger, *Angew. Chem., Int. Ed.*, 2002, **41**, 2281.
- 33 for example F. Yu, D.-D. Li, L. Cheng, Z. Yin, M.-H. Zeng and M. Kurmoo, *Inorg. Chem.*, 2015, **54**, 1655; C. Falaise, C. Volkringre, J. Facqueur, T. Bousquet, L. Gasnot, and T. Loiseau, *Chem. Commun.*, 2013, **49**, 10320; H. Kitagawa, H. Ohtsu, M. Kawano, *Angew. Chem., Int. Ed.*, 2013, **52**, 12395; P. Cui, L. Ren, Z. Chen, H. Hu, B. Zhao, W. Shi, and P. Cheng, *Inorg. Chem.*, 2012, **51**, 2303; M.-H. Zeng, Q.-X. Wang, Y.-X. Tan, S. Hu, H.-X. Zhao, L. S. Long and M. Kurmoo, *J. Am. Chem. Soc.*, 2010, **132**, 2561; D. F. Sava, M. A. Rodriguez, K. W. Chapman, P. J. Chupas, J. A. Greathouse, P. S. Crozier, T. M. Nenoff, *J. Am. Chem. Soc.*, 2011, **133**, 12398; Q.-K. Liu, J.-P. Ma and Y.-B. Dong, *Chem. Commun.*, 2011, **47**, 7185.
- 34 for example S.-S. Liu, S. Yuan, X.-Y. Li, S. Miao, Z.-W. Yu, *Inorg. Chim. Acta*, 2014, **416**, 195; S.-R. Zheng, Q.-Y. Yang, Y.-R. Liu, J.-Y. Zhang, Y.-X. Tong, C.-Y. Zhao and C.-Y. Su, *Chem. Commun.*, 2008, 356; E. Q. Gao, N. Liu, A. L. Cheng and S. Gao, *Chem. Commun.*, 2007, 2470; L. Zhang, Z.-J. Li, Q.-P. Lin, J. Zhang, P.-X. Yin, Y.-Y. Qin, J.-K. Cheng and Y.-G. Yao, *CrystEngComm*, 2009, **11**, 1934; B. Zheng, D. Zhang, Y. Peng, Q. Huo and Y. Liu, *Inorg. Chem. Commun.*, 2012, **16**, 70; P. Cui, J. Wu, X. Zhao, D. Sun, L. Zhang, J. Guo and D. Sun, *Cryst. Growth Des.*, 2011, **11**, 5182; D.-C. Zhong, W.-G. Lu, L. Jiang, X.-L. Feng and T.-B. Lu, *Cryst. Growth Des.*, 2010, **10**, 739; T. Jiang and X.-M. Zhang, *Cryst. Growth Des.*, 2008, **8**, 3077.
- 35 J. A. Hyatt, *J. Org. Chem.*, 1978, **43**, 1808.
- 36 S.P. Schmidt, W. C. Trogler, F. Basolo, M. A. Urbancic and J. R. Shapley, *Inorg. Synth.*, 1990, **28**, 160.
- 37 G. M. Sheldrick, *Acta Crystallogr. A*, 2008, **A64**, 112.
- 38 L. Palatinus and G. Chapuis, *J. Appl. Cryst.*, 2007, **40**, 786.
- 39 A. L. Spek, *Acta Crystallogr. C*, 2015, **C71**, 9.